A refined carrier-to-code levelling method for retrieving ionospheric measurements from dual-frequency GPS data

Xiao Zhang[1,2], **Baocheng Zhang**[1,3], **Yunbin Yuan**[1], **Jiuping Zha**[1,2] and **Min Li**[1]

[1] State Key Laboratory of Geodesy and Earth's Dynamics, Institute of Geodesy and Geophysics, Chinese Academy of Sciences, Wuhan, People's Republic of China
[2] University of Chinese Academy of Sciences, Beijing, People's Republic of China

E-mail: zxwhigg@whigg.ac.cn and b.zhang@whigg.ac.cn

Abstract

The retrieval of ionosphere measurements (IMs) constitutes the first key step in the process of ionospheric monitoring with the global positioning system (GPS). Carrier-to-code levelling (CCL) is one of the most widely used retrieval methods, mainly because of its simplicity and effectiveness. However, CCL-derived IMs have been proven to be susceptible to so-called levelling errors, which is mainly due to the presence of code multipath effects and the occurrence of short-term variability in receiver code biases (RCBs). To address these levelling errors, we propose a refined CCL (rCCL) method, in which the code multipath and RCB variations are jointly estimated as time-varying parameters and thus removed. Compared to the customary CCL method, this new method has two advantages. First, rCCL is able to exclude the effect of code multipath and time-varying RCBs from IMs, thereby greatly reducing the levelling errors of IM estimates. Second, the RCB variations are estimated for each individual code observation using a single receiver, allowing easy and effective calibration of the short-term variability in RCBs and the linear combination of, for instance, receiver differential code biases (rDCBs).

Keywords: global positioning system (gps), ionosphere measurements (ims), code multipath, receiver code biases (rcbs), refined carrier-to-code levelling (rCCL)

(Some figures may appear in colour only in the online journal)

1. Introduction

Total electron content (TEC) is one of the most important ionospheric parameters provided by the global positioning system (GPS) [4, 5, 8, 11]. The first key step in obtaining this parameter is to retrieve ionosphere measurements (IMs); the interpretation of the measurements is widely regarded as the slant TEC (sTEC) along the satellite to receiver line of sight (LOS), contaminated by satellite and receiver differential code biases (DCBs) that commonly assume time invariance over one day. Under this assumption, one can then utilize the thin-layer ionospheric model in the second step to remove DCBs from IMs [17, 20], leaving only the sTEC, which can then be used as input for further ionosphere-related research and applications [9, 13, 18].

This study mainly focuses on the retrieval of IMs from GPS data. GPS carrier-phase observations can offer precise measurements of sTEC variation over time but are biased by arc-dependent ambiguity offsets, hindering the recovery of absolute TEC values unless a large number of arc-dependent ambiguities have been resolved [1]. Thus, it is common practice to fit carrier-phase observations to code observations to remove arc-dependent offsets. This procedure, termed carrier-to-code (CCL), is widely used to generate IMs and

---

[3] Author to whom any correspondence should be addressed.

Table 1. An overview of the GPS data used in this work.

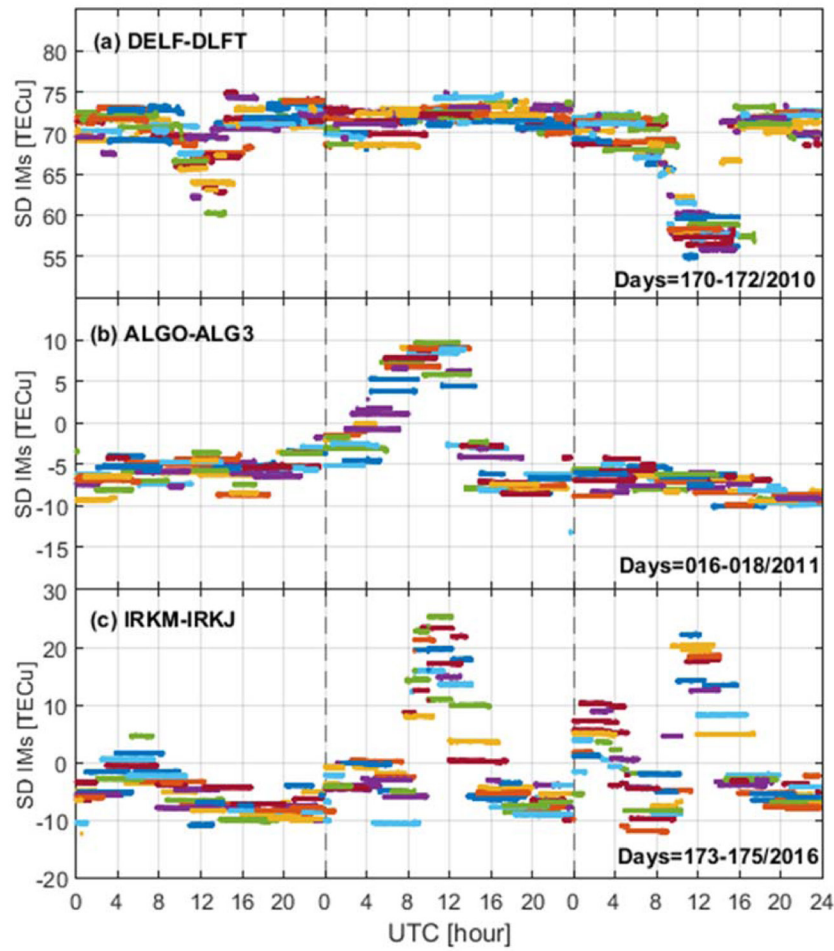| Receiver ID	Receiver type	Antenna type	Location	Observation period
DELF	TRIMBLE 4700 N1.30/S0.00	TRM29659.00 UNAV	51.98°N, 4.38°E	2010, Days 170–172
DLFT	MT311941902 JPS LEGACY	JPSREGANT_DD_E NONE	DELF-DLFT Baseline:12 m	
ALGO	(124-U) AOA BENCHMARK ACT 3.3.32.2N	(386)AOAD/M_T NONE	45.95°N, 78.07°W	2011, Days 016–018
ALG3	(401-01989) TPS NETG3 3.4	(383-0414) TPSCR.G3 NONE	ALGO-ALG3 Baseline:153 m	
IRKJ	00517 JPS LEGACY	RA0225 JPSREGANT_SD_E1 NONE	52.22°N, 104.32°E	2016, Days 173–175
IRKM	LP01756 ASHTECH Z-XII3	AOAD/M_T NONE	IRKJ-IRKM Baseline:3 m	

Figure 1. SD IMs retrieved by CCL method for three pairs of colocated receivers over three consecutive days. Different colours correspond to different satellite arcs. Subplots: (a) DELF-DLFT; (b) ALGO-ALG3; (c) IRKM-IRKJ.

then produce a global ionosphere map (GIM) [10], which is accomplished at most ionospheric associate analysis centers (IAACS) of the International Global Navigation Satellite System (GNSS) Service (IGS). However, compared to carrier-phase observations, code observations are affected much more by observation noise and multipath effects. Moreover, receiver code biases (RCBs) in code observations have been found to vary dramatically on timescales of hours or less [1, 14], which is mainly due to surrounding temperature fluctuations [7, 12]. If the code multipath and RCB variation quantities do not average to zero over a continuous arc, the CCL procedure thereby introduces levelling errors of up to several TEC units (TECu, where one TECu equals 0.162 m at the first GPS frequency) or more in IMs [15, 24]. As reported in [6], the levelling errors induced by code multipath and intra-day variations in RCBs can reach a peak-to-peak amplitude of ±8.8 TECu.

To address the levelling errors, efforts have been made by two representative methods, namely, the uncombined precise point positioning (PPP) technique and the 'integer-levelled' method. The PPP is based on a geometry-based model in which a large set of geometric unknowns have to be extended into less receiver-dependent ones [16, 22], and IMs as one of the outputs can be retrieved along with other parameters,

such as receiver position, receiver clock error and ambiguities. However, to enable PPP, one needs to take full advantage of precise satellite products externally provided, such as satellite orbit and clock errors, which can strengthen the PPP functional model. Hence, the errors in PPP-derived IMs can be greatly reduced [21, 22]. In order to avoid the effect of code bias and multipath on the IMs' retrieval totally, the 'integer-levelled' method is proposed to use the geometry-free phase observations only, in which the unknown ambiguities of the phase observations are corrected directly using the estimated ambiguities by PPP, making the IMs' retrieval virtually free of the errors induced by code multipath and intra-day variations in RCBs [1]. However, the two methods must rely on the support of externally provided precise satellite products, whose latency limits the usefulness of these methods in everyday practice.

With the goal of eliminating the adverse effect of code multipath and intra-day variations in RCBs on IMs in an effective and simple way, we proposed a refined CCL (rCCL) method in which the time-varying RCBs and code multipath are retrieved, modelled and finally removed from the IMs. The effectiveness of this method is that the levelling errors of estimated IMs can be greatly reduced compared with the original CCL method. In addition, its simplicity is demonstrated in
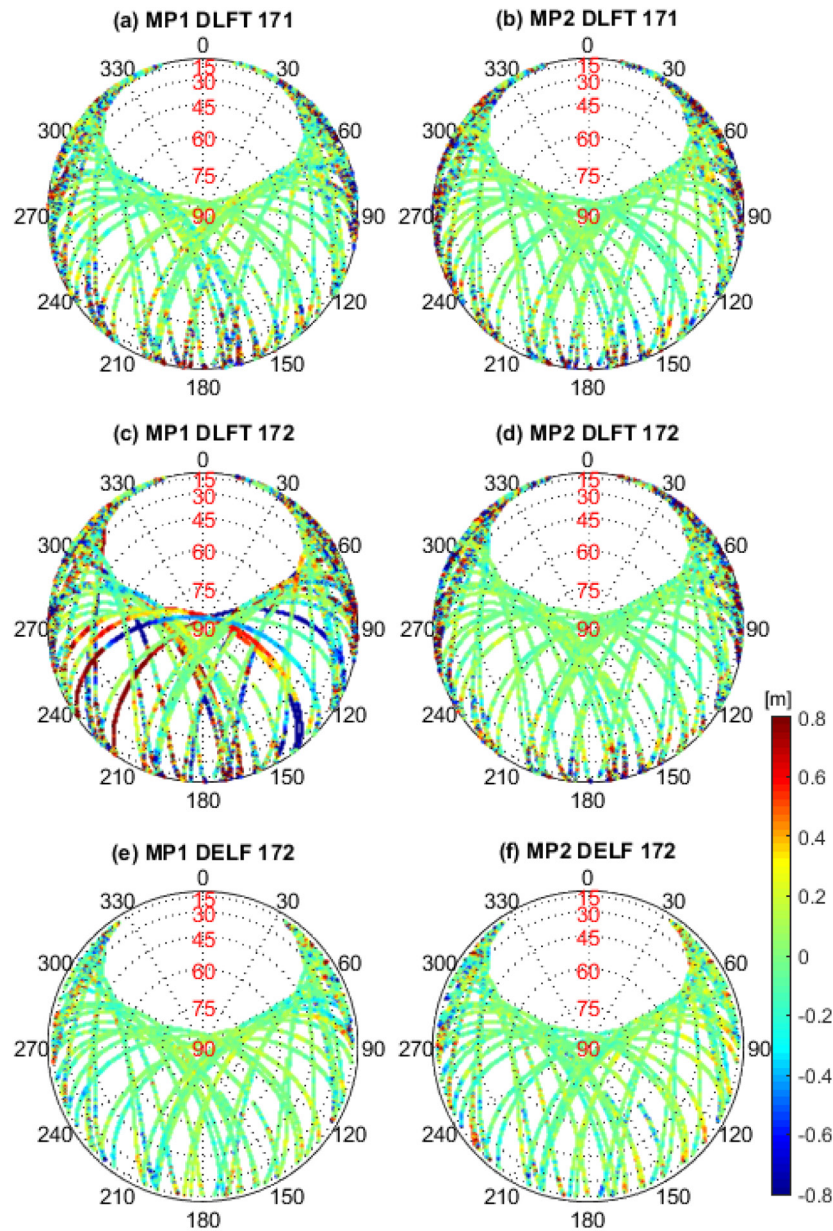
Figure 2. Sky plots of the code multipath observations computed by multipath combination over the receiver DLFT on days 171–172 and receiver DELF on day 172 in 2010. MP1 and MP2 correspond to multipath observations on two individual frequencies. The azimuth angle is measured clockwise from the north. The elevation angle is measured upwards from the ground plane. The centre represents an elevation angle of 90°. The largest circle represents an elevation angle of 0°.

that in comparison with PPP or the integer-levelled method, its implementation does not require precise satellite product support.

The rest of this study is organized as follows. Section 2 presents a brief introduction to the customary CCL method and the levelling errors induced. Then, a new rCCL method is proposed and discussed based on theoretical methodologies. Section 3 demonstrates the numerical results, including the estimated code multipath, RCB variation and IMs determined

with the proposed method. Finally, conclusions are presented in section 4.

2. Methods

In this section, we begin to review briefly the GPS code and carrier phase observations and the CCL method for IMs retrieval. Then, the rCCL method is described in theory, concerning the retrieval, modelling and calibration of the code
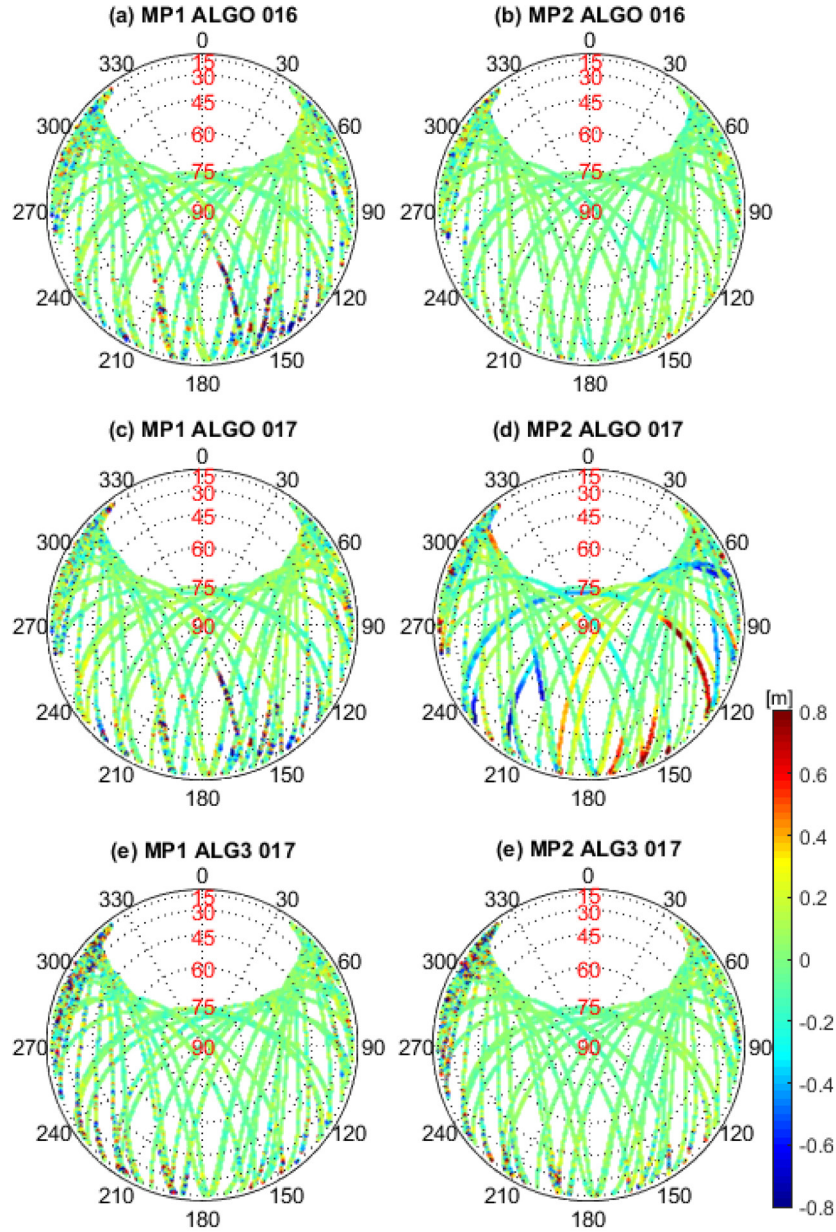
Figure 3. This figure is the same as figure 2 except that it shows the results for the receiver ALGO on days 016–017 and receiver ALG3 on day 017 in 2011.

multipath and intra-day variation in RCBs that degrade the precision of CCL-derived IMs.

2.1. Carrier-to-code levelling (CCL) method

It is well known that code and carrier phase observations of dual-frequency GPS can be briefly described as

$$\varphi_{r,j}^s(i) = \rho_r^s(i) - \mu_j l_r^s(i) + N_{r,j}^s$$
$$p_{r,j}^s(i) = \rho_r^s(i) + \mu_j l_r^s(i) + d_{r,j} - d_j^s \tag{1}$$

where $\varphi_{r,j}^s(i)$ and $p_{r,j}^s(i)$ denote, respectively, the phase and code observations from satellite s to receiver r at epoch i on the frequency of $j = 1, 2$, $\rho_r^s(i)$ refers to the total sum of frequency-independent geometric effects, including the receiver–satellite range, slant tropospheric delay, satellite

clock and receiver clock, $l_r^s(i)$ denotes the slant ionospheric delay with respect to the first frequency f_1, and its coefficient is given by $\mu_j = f_1^2/f_j^2$, $N_{r,j}^s$ is the real-value ambiguity, d_j^s and $d_{r,j}$ denote, respectively, the satellite code bias (SCB) and receiver counterpart (RCB). All the parameters are denoted in units of meters.

In order to avoid the estimation of a large set of geometric effects $\rho_r^s(i)$, the geometry-free (GF) combinations of GPS observations in equation (1) can be constructed as

$$\varphi_{r,gf}^s(i) = \varphi_{r,1}^s(i) - \varphi_{r,2}^s(i)$$
$$= (\mu_2 - \mu_1) \cdot l_r^s(i) + N_{r,1}^s - N_{r,2}^s$$
$$p_{r,gf}^s(i) = p_{r,1}^s(i) - p_{r,2}^s(i)$$
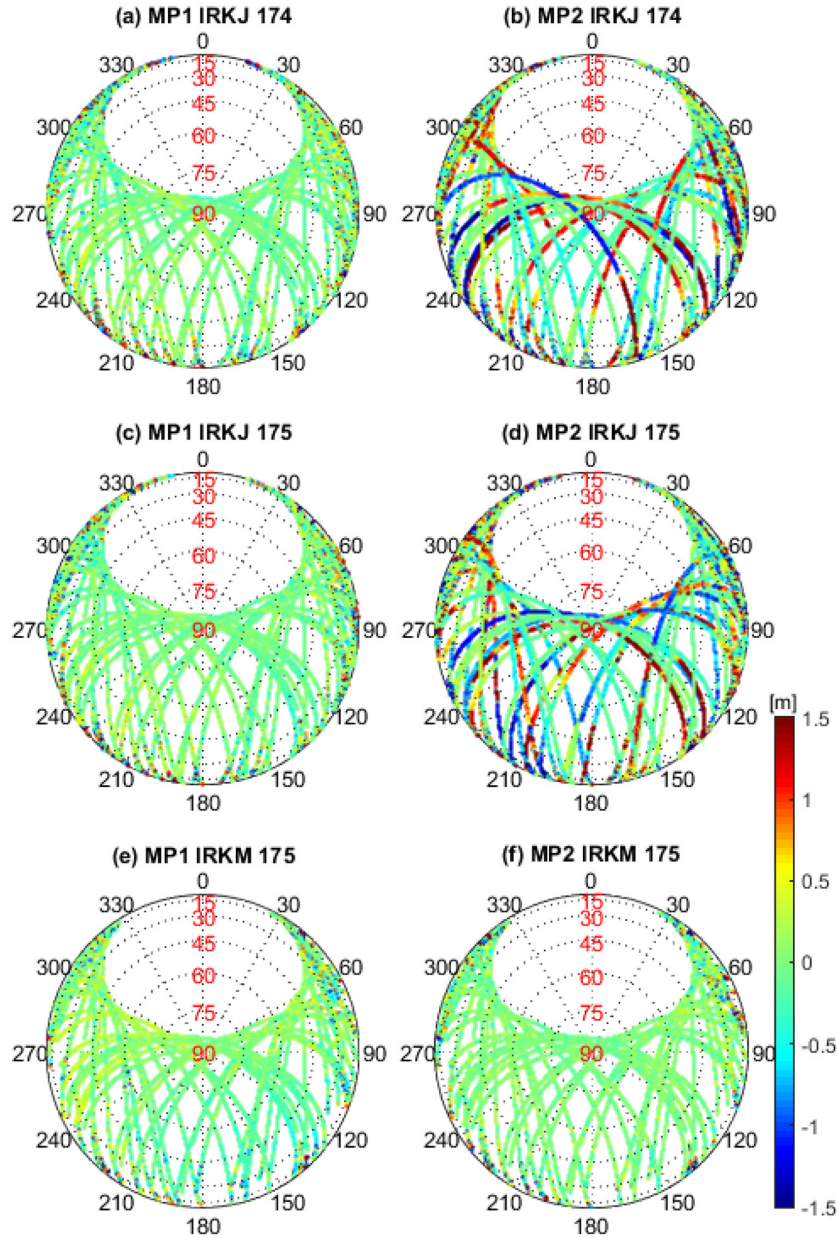$$= (\mu_1 - \mu_2) \cdot l_r^s(i) - d_{,gf}^s + d_{r,gf} \tag{2}$$

Figure 4. This figure is the same as figure 2 except that it shows the results for receiver IRKJ on days 174–175 and receiver IRKM on day 175 in 2016.

where $d_{,gf}^s = d_{,1}^s - d_{,2}^s$ and $d_{r,gf} = d_{r,1} - d_{r,2}$ denote, respectively, satellite and receiver differential code bias (DCB).

As equation (2) shows, except that $l_r^s(i)$ can change between epochs, the remaining parameters are assumed constant over time. This assumption thereby makes the retrieval of IMs using the 'carrier-to-code levelling' (CCL) process possible, which mainly involves two steps: first, provided that a continuous satellite arc consists of a total of T epochs, (weighted) averaging $\varphi_{r,gf}^s(i) + p_{r,gf}^s(i)$ over T epochs can yield a levelling constant c_r^s, which amounts to $N_{r,1}^s - N_{r,2}^s - d_{,gf}^s + d_{r,gf}$. Then, subtracting $\varphi_{r,gf}^s(i)$ from c_r^s, a set of IMs can be obtained, which reads

$$\bar{l}_r^s(i) = l_r^s(i) + \frac{1}{(\mu_1 - \mu_2)}(d_{r,gf} - d_{,gf}^s) \qquad (3)$$

where $\bar{l}_r^s(i)$ is the CCL-derived IMs.

However, it should be noted that, in the CCL process, the estimation of levelling constant c_r^s would be subjected to the code multipath effect on $p_{r,gf}^s(i)$ and possible short-term variability in receiver DCB $d_{,gf}^s$, neither of which can be fully averaged out over a continuous arc, resulting in an arc-dependent bias in c_r^s, called 'levelling errors', that eventually enter the CCL-derived IMs, $\bar{l}_r^s(i)$.

To evaluate the magnitude of levelling errors, one typical way is the short- and zero-baseline experiment of two colocated receivers [6], in which their slant ionospheric delays are considered identical, namely $l_p^s(i) = l_q^s(i)$. Thus, according to equation (3), the single-difference (SD) IMs of the two receivers can be obtained by
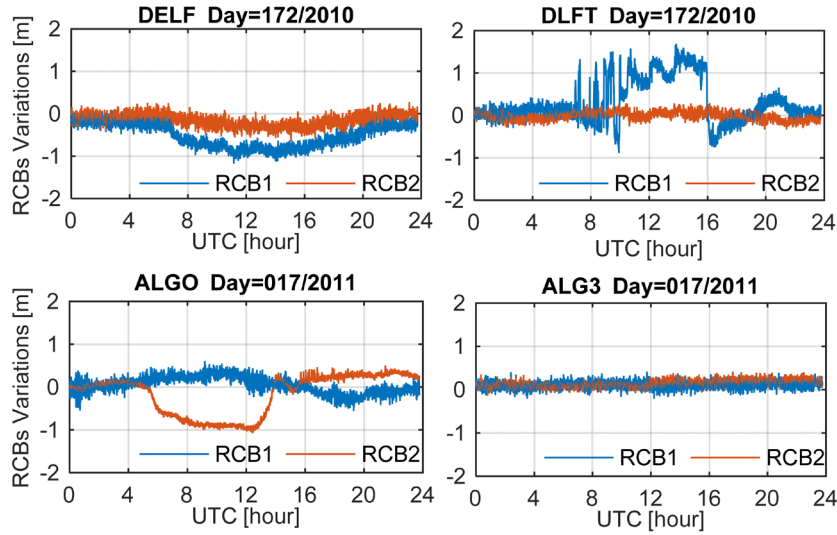
Figure 5. The RCB variations estimated using rCCL for receivers DELF, DLFT, ALGO and ALG3 over one day. RCB1 (blue line) and RCB2 (red line) correspond to the RCB variations on two individual frequencies.
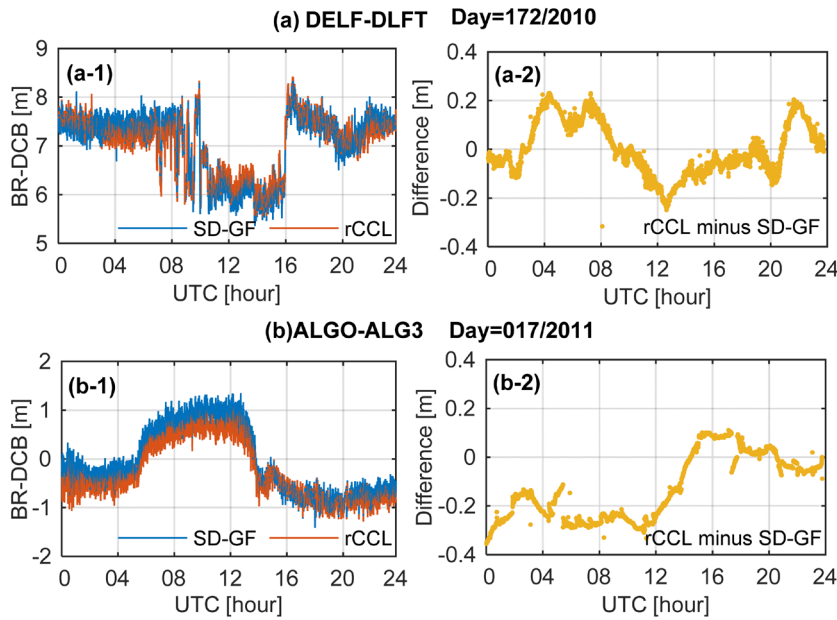

Figure 6. Epoch-by-epoch estimates of BR-DCB using SD-GF method (blue line) and rCCL method (red line) for two pairs of colocated receivers over one day；the differences between SD-GF and rCCL estimates (yellow dots); subplots: (a) DELF-DLFT; (b) ALGO-ALG3.

$$\Delta \bar{l}_{pq}^{s}(i) = \bar{l}_{p}^{s}(i) - \bar{l}_{q}^{s}(i) = \frac{1}{(\mu_1 - \mu_2)}(d_{p,gf} - d_{q,gf}) \quad (4)$$

where $\Delta \bar{l}_{pq}^{s}(i)$ denote SD IMs, $\bar{l}_{p}^{s}(i)$ and $\bar{l}_{q}^{s}(i)$ denote the IMs of receivers p and q, $d_{q,gf} - d_{p,gf}$ denote the between-receiver DCB (BR-DCB).

In theory, the SD IMs across all satellite arcs, interpreted BR-DCB, should be one common value. However, due to the effects of observation noise, code multipath and receiver DCB variation, the SD IMs of different satellite arcs would exhibit discrepancies, which thus allows the assessment of the magnitude of levelling errors [6].

2.2. Refined CCL (rCCL) method

Taking the receiver code bias variation and multipath effect into consideration, we reformulate equation (1) as

$$\varphi_{r,j}^{s}(i) = \rho_{r}^{s}(i) - \mu_j l_{r}^{s}(i) + N_{r,j}^{s}$$
$$p_{r,j}^{s}(i) = \rho_{r}^{s}(i) + \mu_j l_{r}^{s}(i) - d_{j}^{s} + d_{r,j}(i) + m_{r,j}^{s}(i) \quad (5)$$

with the newly-defined RCB $d_{r,j}(i)$ and code multipath $m_{r,j}^{s}(i)$ on frequency j, both of which are allowed to change between epochs.

Obviously, in equation (5), the number of its observations is insufficient compared with unknown parameters. To
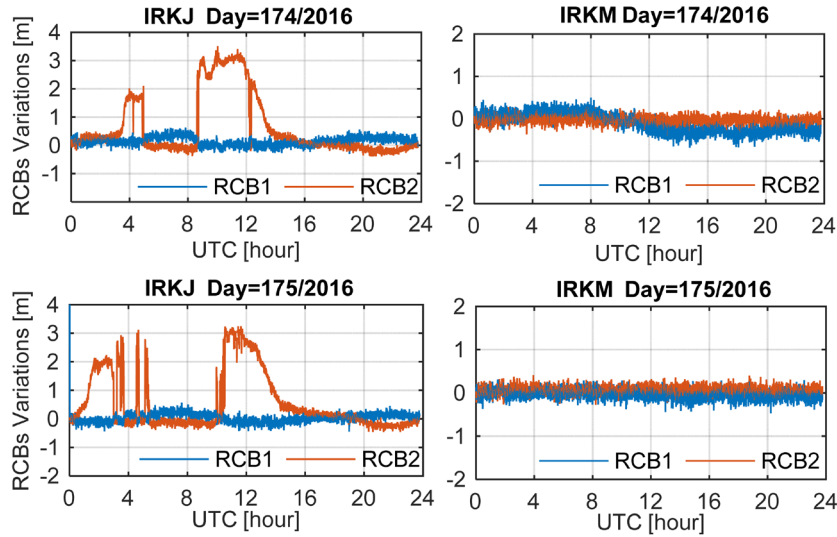
Figure 7. The RCB variations estimated using rCCL for receivers IRKJ and IRKM over two days. RCB1 (blue line) and RCB2 (red line) correspond to the RCB variations on two individual frequencies.
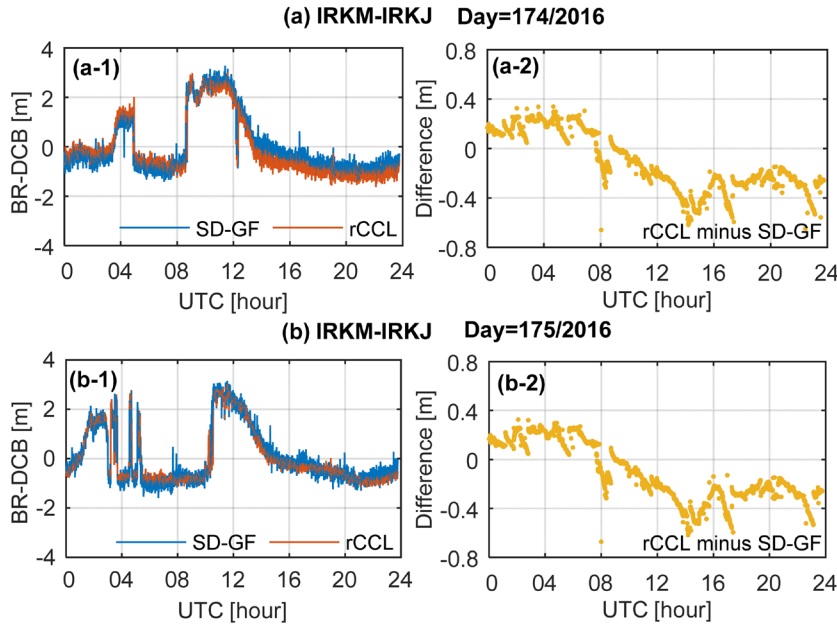

Figure 8. Epoch-by-epoch estimates of BR-DCB using SD-GF method (blue line) and rCCL method (red line) for the colocated receivers IRKM and IRKJ over days 174 and 175; the differences between SD-GF and rCCL estimates (yellow dots).

solve this, we first construct a linear combination of single-frequency code and dual-frequency phase observations, called multipath combination observation (MP) [2, 19], which reads,

$$
\begin{aligned}
MP^s_{r,j}(i) &= p^s_{r,j}(i) - \varphi^s_{r,j}(i) + \frac{2\mu_j}{\mu_1 - \mu_2}\left(\varphi^s_{r,1}(i) - \varphi^s_{r,2}(i)\right) \\
&= m^s_{r,j}(i) + \mathrm{d}r, j_{r,j}(i) + b^s_{r,j}
\end{aligned}
\tag{6}
$$

with

$$
b^s_{r,j} = -N^s_{r,j} - d^s_j + \frac{2\mu_j}{\mu_1 - \mu_2}(N^s_{r,1} - N^s_{r,2}).
\tag{7}
$$

Equation (6) represents a rank-deficient system, in which the unknown parameters are not individually estimable, but only combinations of them. The first type of rank deficiencies, whose size equals the number of satellites, occurs between $m^s_{r,j}(i)$ and $b^s_{r,j}$. We solve this by representing $m^s_{r,j}(i)$ with spherical harmonic functions of the azimuth and elevation angle of satellites. The second type of rank deficiencies, occurring between $d_{r,j}(i)$ and $b^s_{r,j}$, is of size one. It is solvable by choosing $d_{r,j}(1)$, the RCB associated with the first (reference) epoch, as datum, and recombining the datum with other parameters. Having eliminated the rank deficiencies, the full-rank version of equation (6) now reads

$$
\begin{aligned}
MP^s_{r,j}(i) = \sum_{n=0}^{3}\sum_{m=0}^{n} P_{nm}\left(\sin(e)\right)\left(\alpha_{nm}\cos(m\cdot a)\right. \\
\left. + \beta_{nm}\sin(m\cdot a)\right) + \Delta d_{r,j}(i) + \bar{b}^s_{r,j}
\end{aligned}
\tag{8}
$$

with

Figure 9. The time series of code multipath observations with (right panels) and without (left panels) RCB corrections for GPS satellites PRN06, PRN12 and PRN17, tracked by the receiver ALGO on days 16 (blue line) and 17 (red line) in 2011.
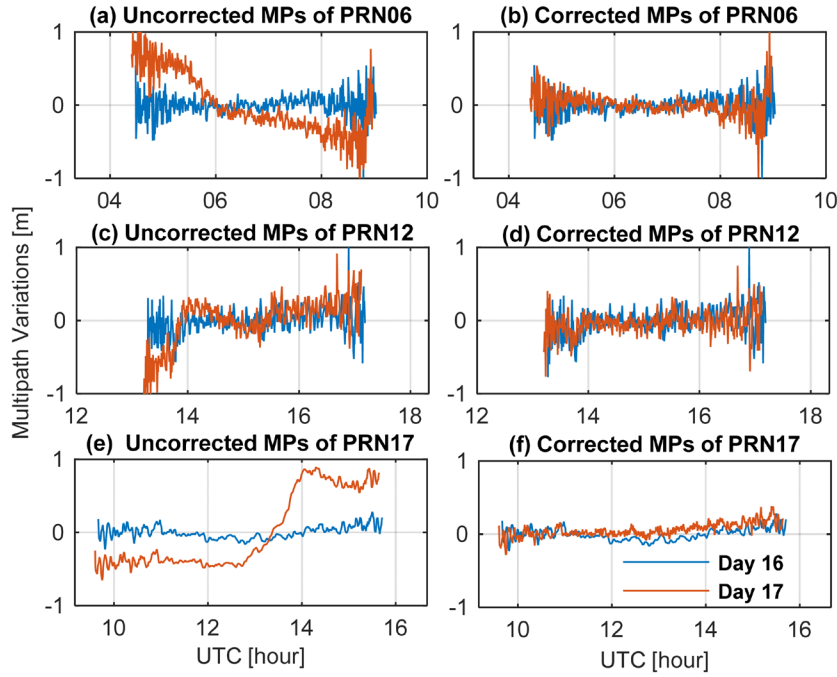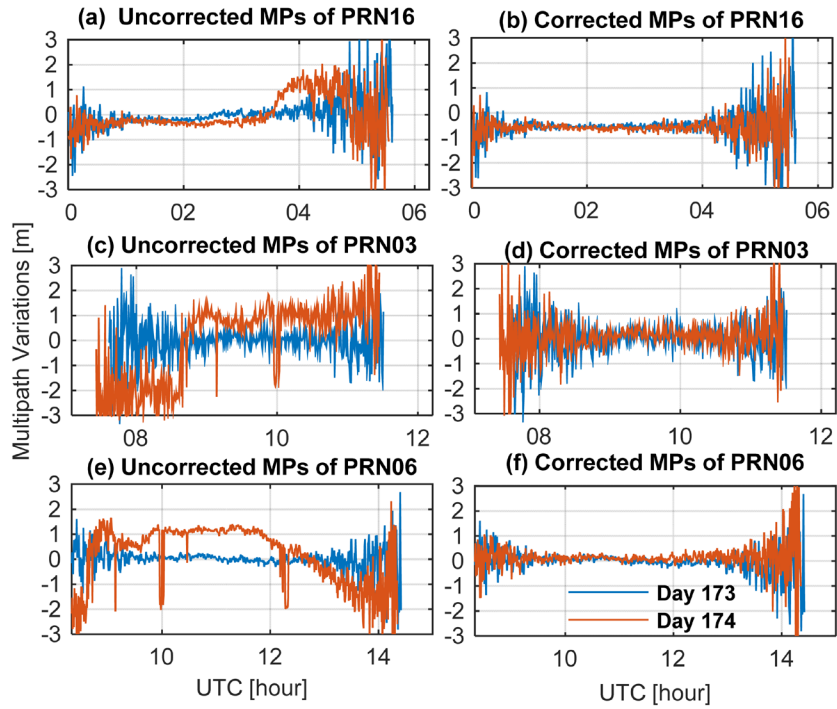

Figure 10. The time series of code multipath observations with (right panels) and without (left panels) RCB corrections for GPS satellites PRN16, PRN03 and PRN06, tracked by receiver IRKJ on days 173 (blue line) and 174 (red line) in 2016.

$$\Delta d_{r,j}(i) = d_{r,j}(i) - d_{r,j}(1)$$
$$\bar{b}_{r,j}^{s} = b_{r,j}^{s} + d_{r,j}(1) \tag{9}$$

where $MP_{r,j}^{s}(i)$ encompasses now a vector of multipath combination observations for the satellites tracked by a single receiver at epoch i, the $P_{nm}(\cdot)$ denotes the Legendre polynomial, a and e denote, respectively, the azimuth and elevation angles of the satellite. The remaining parameters are estimable, including spherical harmonic coefficients α_{nm} and β_{nm}, the RCB variations $\Delta d_{r,j}(i)$ ($\Delta d_{r,j}(1) = 0$) and the constant biases $\bar{b}_{r,j}^{s}$. As far as equation (8) is concerned, at the initial epoch, the number of observations is insufficient compared with the unknowns of this model. By cumulating the observations over several epochs, the least squares solutions of the
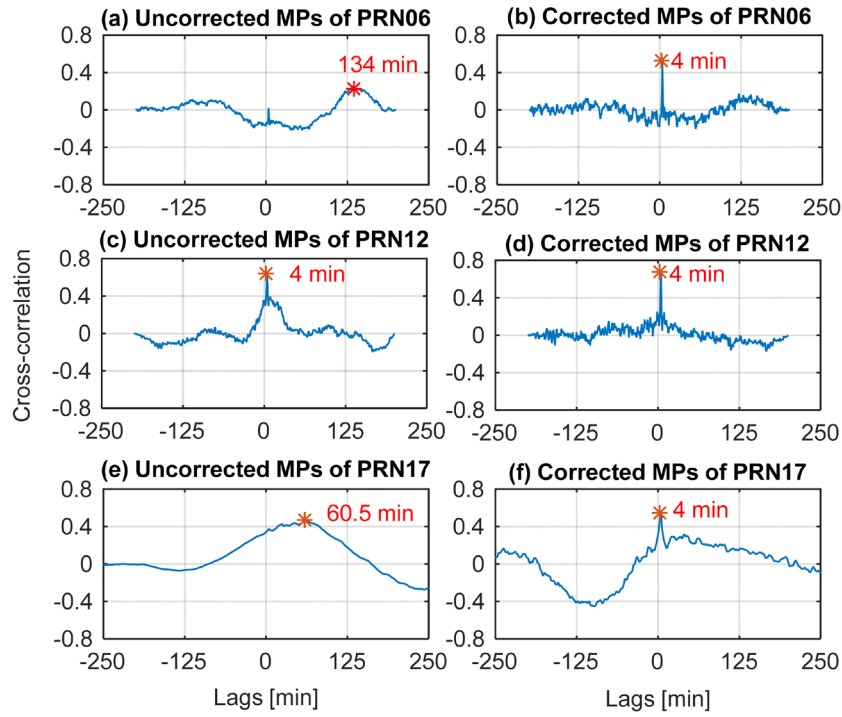
Figure 11. Cross-correlations between the multipath time series of two consecutive days for the GPS satellites PRN06, PRN12 and PRN17, tracked by receiver ALGO on days 16 and 17 in 2011, with the red asterisk indicating the maximum of cross-correlations between two time series shown in figure 9.
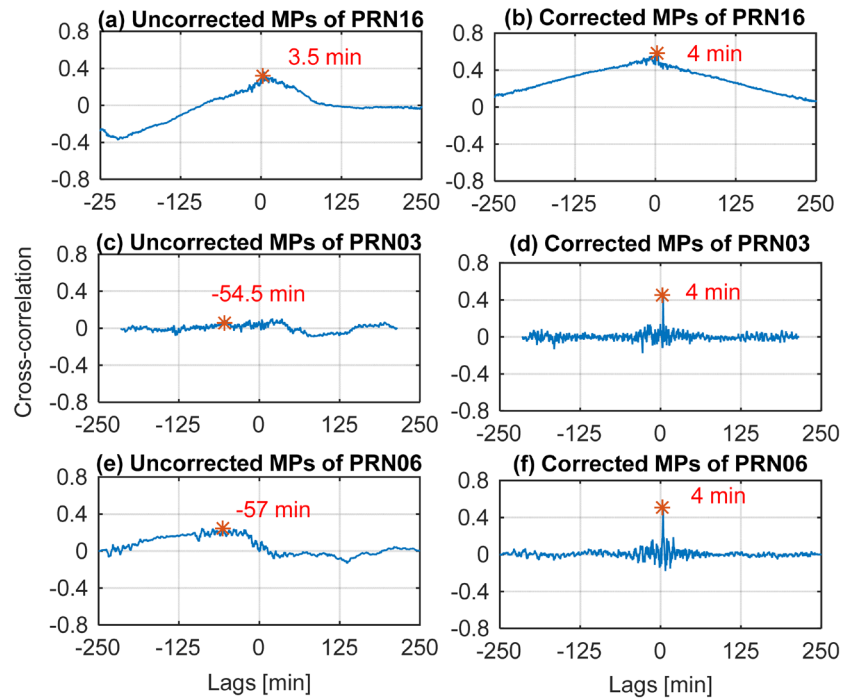
Figure 12. Cross-correlations between the multipath time series of two consecutive days for the GPS satellites PRN16, PRN03 and PRN06, tracked by receiver IRKJ on days 173 and 174 in 2016, with the red asterisk indicating the maximum of cross-correlations between two time series shown in figure 10.
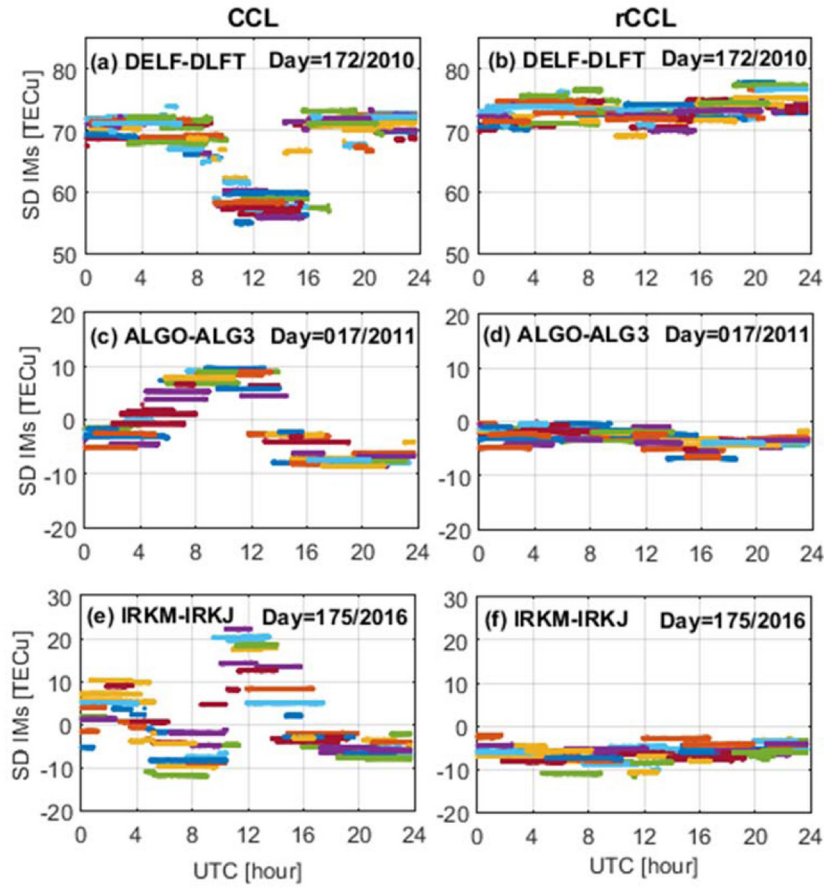
Figure 13. SD IMs for three pairs of colocated receivers over one representative day. The left panels are the CCL results, and the right panels are the rCCL results.

unknown parameters can be obtained and used as the initial values for the subsequent Kalman filter.

On the basis of estimated $\Delta d_{r,j}(i)$ (epoch-wise estimates) and $m_{r,j}^s(i)$ (interpreted as spherical harmonics functions), we can correct the short-term variability in the RCB and code multipath effect on $p_{r,j}^s(i)$ in equation (4), and further construct the GF combination observations, which can take the form

$$
\begin{aligned}
\varphi_{r,gf}^s(i) &= (\mu_2 - \mu_1) \cdot l_r^s(i) + N_{r,1}^s - N_{r,2}^s \\
\tilde{p}_{r,gf}^s(i) &= (\mu_1 - \mu_2) \cdot l_r^s(i) - d_{,gf}^s + d_{r,gf}(1)
\end{aligned}
\tag{10}
$$

where $\tilde{p}_{r,gf}^s(i)$ is the GF code observation with multipath and receiver RCB variation corrections, $d_{r,gf}(1) = d_{r,1}(1) - d_{r,2}(1)$ is the receiver DCB at the first epoch.

Then, applying equation (10) to the 'carrier-to-code levelling' process as section 2.1 gives

$$
\tilde{l}_r^s(i) = l_r^s(i) + \frac{1}{(\mu_1 - \mu_2)} \left(d_{r,gf}(1) - d_{,gf}^s \right)
\tag{11}
$$

in which $\tilde{l}_r^s(i)$ is the IM that refined CCL (rCCL) provided.

Comparing with the CCL method, the IMs retrieval using rCCL first corrects the code multipath effect instead of ignoring it directly. Secondly, the rCCL-derived IMs $\tilde{l}_r^s(i)$ contain, among others, the receiver DCB at the first epoch $d_{r,gf}(1)$ that is reasonable to be constant over time. Thus, the

rCCL-derived IMs can be immune to the levelling errors due to the code multipath effect and short-term variability in the RCB.

3. Results and analysis

This section begins with a brief introduction to the experimental setup for the GPS data collection, which consists of three groups of colocated receivers. For each group, the levelling errors of the CCL-derived IMs are demonstrated. Focusing on the receivers associated with significant levelling errors, we retrieve their code multipath and RCB variations by the proposed rCCL method, aiming to calibrate their code observations. Finally, to validate the rCCL method, we evaluate the levelling errors of the rCCL-derived IMs.

3.1. Experimental setup

Table 1 presents an overview of the experimental data sets measured by three groups of colocated receivers over three consecutive days, with a sampling rate of 30 s and a cutoff elevation angle of 5°. Each pair of colocated receivers can form one short-baseline, with lengths between approximately 3 m and 153 m, implying that in a SD model between receivers,
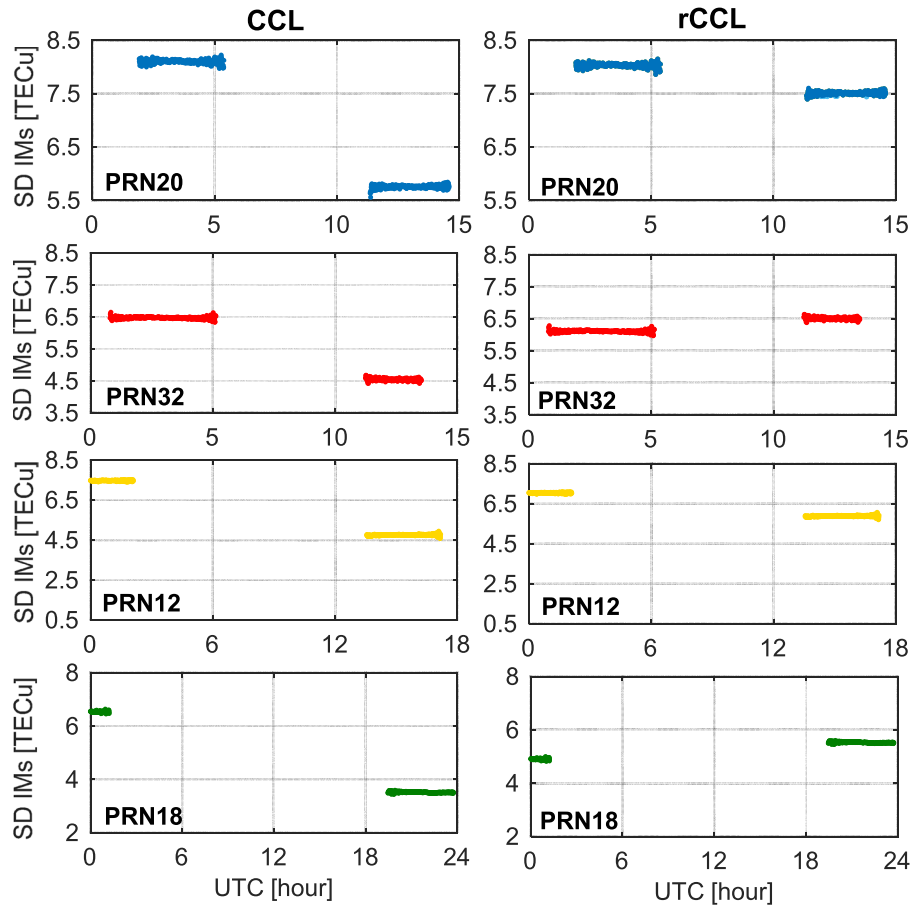
Figure 14. SD IMs between receivers ALGO and ALG3 on day 17 in 2011 for the GPS satellites PRN20, PRN32, PRN12 and PRN18, which have two arcs over one day. The left panels are the CCL results, and the right panels are the rCCL results.

atmospheric errors and satellite-dependent errors are absent. The first and second sets of data were used in [1, 14], respectively, to exhibit significant intra-day variations in rDCB that resulted in the presence of levelling errors; the third set of data is selected to present a statistically representative result.

The GPS datasets were processed on a daily basis with the following strategies: (1) the elevation-dependent weighting function was applied to alleviate noisy observations [22], in which the zenith-referenced standard deviation was set to 30 cm for the code and 0.3 cm for the phase. (2) The broadcast ephemeris was used to compute the satellite positions. (3) The turbo edit method was used to identify the cycle slips [3]. When cycle slips occur, the arc is split into two arcs for processing. (4) The arcs containing at least 60 epochs (i.e. 0.5 h) were retained to retrieve the IMs.

3.2. Assessment of levelling errors

Figure 1 shows the SD IMs retrieved by the CCL method for three pairs of colocated receivers over three consecutive days, in which different colours represent different satellites. As stated earlier, the SD IMs between two closer receivers for all satellite arcs, in theory, should be one common value. However, it can be seen that from subplot (a) to subplot (c), the arc-to-arc spreads reach peak-to-peak values of almost 18.5, 20.0 and 35.4 TECu, respectively. Moreover, for each receiver-pair

configuration, the significant spreads of SD IMs do not repeat over three consecutive days, suggesting that these spreads are not completely dominated by multipath effects. According to equation (4), this variation could be attributed to the instabilities of the RCBs. However, on the basis of these results alone, it is difficult to identify the receivers whose RCBs fluctuate significantly during the course of the three days.

To solve this limitation, figures 2–4 display sky plots of the multipath combination observation (MPs) variations. The raw MPs contain, among other parameters, the lumped biases $b_{r,j}^s$ of phase ambiguities and satellite code bias as equation (5) shows. These lumped biases will reach considerable large values which are determined as an average over raw MP values for each continuous satellite arc and removed from the raw MPs [19]. As a consequence, MP variations can be obtained, which are our main interest, reflecting multipath effects and RCB variation on individual frequency. MP1 and MP2 denote the MPs' variations of the GPS P1-code and P2-code observations, respectively.

Taking the sky plots of receivers DLFT and DELF in figure 2 as an example, MP1 of receiver DLFT presents different distributions over two consecutive days (figures 2(a) and (c)), while MP2 show similarities over the same period (figures 2(b) and (d)). In particular, on day 172, MP1 shows a significant variation, with a peak-to-peak range of almost 1.6 m. At the same time, the distributions of receiver DELF
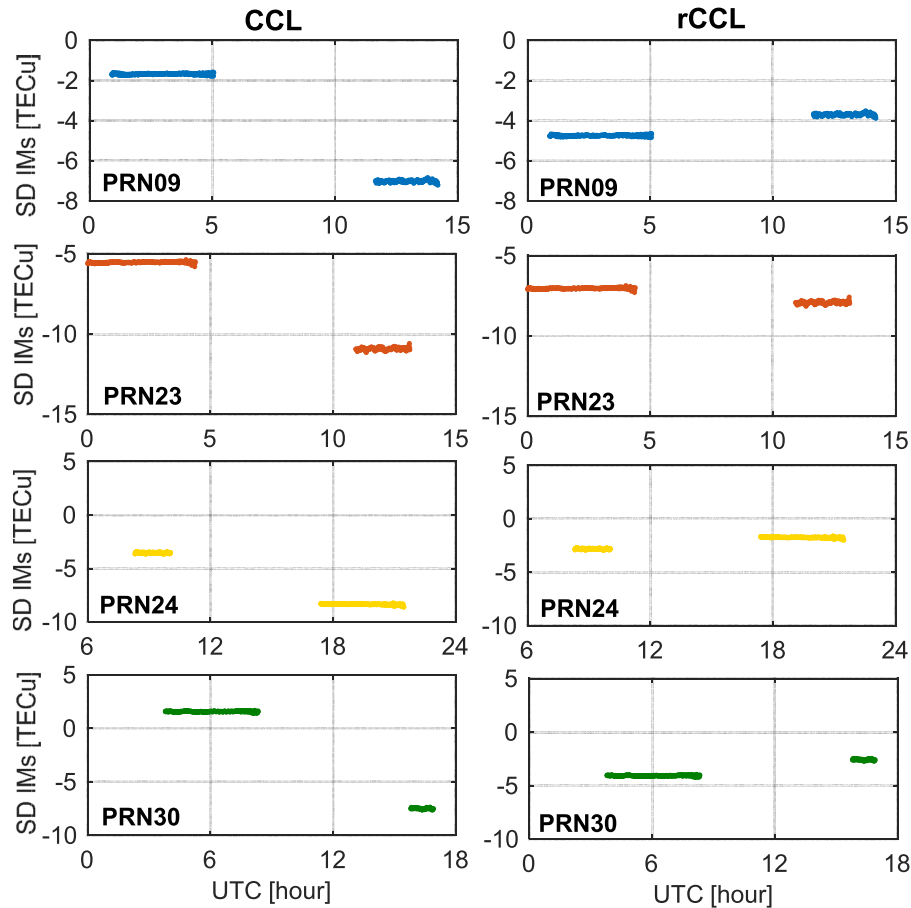
Figure 15. SD IMs between receivers IRKM and IRKJ on day 175 in 2016 for the GPS satellites PRN09, PRN23, PRN24 and PRN30, which have two arcs over one day. The left panels are the CCL results, and the right panels are the rCCL results.

do not exhibit obvious changes. Clearly, the SD IMs spread at day 172, as shown in figure 1(a), can be attributed to the significant variation in MP1 of receiver DLFT. Figures 3 and 4 are analogous to figure 2. The MP2 of receiver ALGO on day 17 (figure 3(d)) and the MP2 of receiver IRKJ on days 174 and 175 (figures 4(b) and (d)) clearly vary during the period, while ones from receivers ALG3 (figure 3(f)) and IRKM (figure 4(f)) are rather constant. We can therefore conclude that the substantial levelling errors, as shown in figures 1(b) and (c), originate mainly from P2-code observations.

3.3. Estimation of time-varying RCBs and code multipath

From the analysis previously presented, we have identified the error source of the significant levelling errors of SD IMs. For the code observations identified, the time-varying RCBs and code multipath can be jointly estimated by the rCCL method using equation (8). Figure 5 shows the results of the estimated RCB variations, which are represented, respectively, with RCB1 and RCB2, according to their frequencies. We can see that RCB1 of receiver DLFT exhibits a substantial intra-day variation, while the one of receiver DELF also clearly varies during the day. In comparison, their RCB2 is relatively constant. For the receivers ALGO and ALG3, the RCB2 of the ALGO exhibits a 'U-shape' variation, while the variations are evident for neither RCB1 nor RCB2 of receiver ALG3.

To verify the correctness of these estimates further, the time-wise BR-DCB as a reference are also computed using SD-GF code observations according to [23]. As shown in figure 6, blue line denotes the BR-DCB estimates using SD-GF method, which can be considered between-receiver DCB together with code multipath effect; Red line denotes the BR-DCB combined by estimated RCB using rCCL method. We can see that the blue line, in general, agrees well with the red line, especially, showing the same 'U-shape' variation characteristics as the BR-DCB estimates. However, there also exist a few discrepancies shown in the left panels and denoted by yellow dots, interpreted as the code multipath effect on SD-GF code observations. Figure 7 (figure 8) is analogous to figure 5 (figure 6) but is obtained from the data of the other receiver pair, IRKM-IRMJ. There is also good agreement between the estimated RCB variations and the BR-DCB changes, leading to the same conclusion.

Complementarily, we compare the MPs' variations with and without RCB corrections. Because the GPS satellite and static receiver geometries repeat every sidereal day, the multipath effects should recur after one sidereal day (approximately 4 min daily shift). Clearly, as figure 9 (figure 10) show, for three satellites tracked by receiver ALGO (IRKJ), the MPs' variations with the RCB corrections (right panels) show more similar patterns over two consecutive days (red and blue line denote, respectively, the MP time series of two consecutive

days) than those uncorrected (left panels). To further confirm this assertion, the cross-correlations are computed and shown in figure 11 (figure 12). The maximum correlations with the corresponding time tag are marked by red asterisks. For uncorrected multipath observations, the time tag of their maximum correlations is arbitrary. In comparison, the correlations of the corrected multipath observations achieve maximum values when the time tag equals approximately 4 min. The comparison results indicate that the proposed rCCL method is feasible and effective for isolating RCB variations and the code multipath.

3.4. Analysis of the rCCL-derived IMs

On the basis of estimated RCB variation and code multipath, the code observations can be corrected according to equation (11). In this section, we base our analysis on the levelling errors of SD IMs between two colocated receivers, and for the sake of brevity, exhibit only the results for one day, which are representative of all the results that we have obtained. Figure 13 shows the SD IMs retrieved for different satellites using the CCL and rCCL method. The panels from left to right show that the arc-to-arc scatter has been greatly reduced, implying the rCCL-derived IMs are subjected to less levelling errors compared with the CCL method.

For details, the SD IMs of the individual satellites during different periods are also demonstrated in figures 14 and 15, in which the arc-to-arc vertical interval decreases significantly from left to right in the subplots. The reasoning for this is that the levelling errors of the CCL-derived IMs manifest themselves as arc-to-arc scatters due to multipath effects and the intra-day variations in RCBs. Using the rCCL method, the possible multipath effects and RCB variations can be estimated and then calibrated, thus having no impact on the IMs retrieved, resulting in levelling errors that are reasonably smaller.

4. Conclusions

In this paper, we proposed a rCCL method for retrieving IMs. This method includes three sequential procedures. First, the combined effects of code multipath and time-varying RCBs were extracted using multipath combination. Second, we extended the multipath hemispherical model to isolate the RCB variations from the multipath combination observables by introducing new time-varying parameters and reconstructing the model into its full-rank form. Finally, the estimated code multipath and RCB variations were calibrated from the CCL-derived IMs. The contributions of this work include two aspects.

First, in contrast with the customary CCL method, rCCL can provide IMs that are less prone to levelling errors induced by code multipath and RCB fluctuations. This result mainly manifests from the arc-to-arc scatter of SD rCCL-derived IMs being greatly reduced compared with CCL-derived IMs for either different satellites during the same period or the same satellite during different periods.

Second, the rCCL method can provide RCB variations with respect to the first epoch, making it possible to detect the epoch-wise fluctuations in RCBs simply and effectively. This simplicity holds because its implementation only requires a single receiver and does not require zero- or short-baseline setup. The effectiveness lies in the fact that the rCCL-derived RCB variations show good agreement with the BR-DCB characterization provided by the short-baseline method, and the multipath combination observable correlation between two consecutive days, after RCB calibration, can reach a maximum value when the time lag is 4 min. More interestingly, the RCB variations were estimated for each individual code measurement; hence, our results can be easily extended to the uncombined PPP (UCPPP) model.

ORCID iDs

Xiao Zhang ⓘ https://orcid.org/0000-0003-3544-8035
Baocheng Zhang ⓘ https://orcid.org/0000-0001-5006-1432

References

[1] Banville S and Langley R B 2011 Defining the basis of an 'Integer-Levelling' procedure for estimating slant total electron content *Proc. of the 24th Int. Technical Meeting of the Satellite Division of the Institute of Navigation (ION GNSS 2011)* pp 2542–51
[2] Bishop G and Holland E 1994 Multipath impact on ground-based global positioning system range measurements: aspects of measurement, modeling, and mitigation *Agard Conf. Proc. Agard CP* p 29
[3] Blewitt G 1990 An automatic editing algorithm for GPS data *Geophys. Res. Lett.* **17** 199–202
[4] Brunini C and Azpilicueta F J 2009 Accuracy assessment of the GPS-based slant total electron content *J. Geod.* **83** 773–85
[5] Choi B K, Park J U, Roh K M and Lee S J 2013 Comparison of GPS receiver DCB estimation methods using a GPS network *Earth Planets Space* **65** 707–11
[6] Ciraolo L, Azpilicueta F, Brunini C, Meza A and Radicella S M 2007 Calibration errors on experimental slant total electron content (TEC) determined with GPS *J. Geod.* **81** 111–20
[7] Coster A, Williams J, Weatherwax A, Rideout W and Herne D 2013 Accuracy of GPS total electron content: GPS receiver bias temperature dependence *Radio Sci.* **48** 190–6
[8] Hernandez-Pajares M, Juan J M and Sanz J 1999 New approaches in global ionospheric determination using ground GPS data *J. Atmos. Sol.-Terr. Phy.* **61** 1237–47
[9] Hernandez-Pajares M, Juan J M, Sanz J, Aragon-Angel A, Garcia-Rigo A, Salazar D and Escudero M 2011 The ionosphere: effects, GPS modeling and the benefits for space geodetic techniques *J. Geod.* **85** 887–907

[10] Hernandez-Pajares M, Juan J M, Sanz J, Orus R, Garcia-Rigo A, Feltens J, Komjathy A, Schaer S C and Krankowski A 2009 The IGS VTEC maps: a reliable source of ionospheric information since 1998 *J. Geod.* **83** 263–75

[11] Hernandez-Pajares M, Roma-Dollase D, Garcia-Fernandez M, Orus-Perez R and Garcia-Rigo A 2018 Precise ionospheric electron content monitoring from single-frequency GPS receivers *GPS Solut.* **22** 102

[12] Kao S, Tu Y, Chen W, Weng D J and Ji S Y 2013 Factors affecting the estimation of GPS receiver instrumental biases *Surv. Rev.* **44** 59–67

[13] Komjathy A, Galvan D A, Stephens P, Butala M D, Akopian V, Wilson B, Verkhoglyadova O, Mannucci A J and Hickey M 2012 Detecting ionospheric TEC perturbations caused by natural hazards using a global network of GPS receivers: the Tohoku case study *Earth Planets Space* **64** 1287–94

[14] Li M, Yuan Y B, Wang N B, Liu T and Chen Y C 2018 Estimation and analysis of the short-term variations of multi-GNSS receiver differential code biases using global ionosphere maps *J. Geod.* **92** 889–903

[15] Li W, Wang G X, Mi J Z and Zhang S C 2019 Calibration errors in determining slant Total Electron Content (TEC) from multi-GNSS data *Adv. Space Res.* **63** 1670–80

[16] Liu T, Zhang B C, Yuan Y B and Li M 2018 Real-Time Precise Point Positioning (RTPPP) with raw observations and its application in real-time regional ionospheric VTEC modeling *J. Geod.* **92** 1267–83

[17] McCaffrey A M, Jayachandran P T, Themens D R and Langley R B 2017 GPS receiver CODE bias estimation: a comparison of two methods *Adv. Space Res.* **59** 1984–91

[18] Park J, von Frese R R B, Grejner-Brzezinska D A, Morton Y and Gaya-Pique L R 2011 Ionospheric detection of the 25 May 2009 North Korean underground nuclear test *Geophys. Res. Lett.* **38** L22802

[19] Simsky A 2006 Three's the charm: triple-frequency combinations in future GNSS *Inside GNSS* **1** 38–41

[20] Wang N B, Yuan Y B, Li Z S, Montenbruck O and Tan B F 2016 Determination of differential code biases with multi-GNSS observations *J. Geod.* **90** 209–28

[21] Zhang B C 2016 Three methods to retrieve slant total electron content measurements from ground-based GPS receivers and performance assessment *Radio Sci.* **51** 972–88

[22] Zhang B C, Ou J K, Yuan Y B and Li Z S 2012 Extraction of line-of-sight ionospheric observables from GPS data using precise point positioning *Sci. China Earth Sci.* **55** 1919–28

[23] Zhang B C and Teunissen P J G 2015 Characterization of multi-GNSS between-receiver differential code biases using zero and short baselines *Sci. Bull.* **60** 1840–9

[24] Zhao W, Zhang Z X, Zhao J X, Zhu Y H and Zhao J 2015 An ionosphere TEC monitoring method based on real-time multipath error estimation *Proc. of the 28th Int. Technical Meeting of the Satellite Division of the Institute of Navigation (ION GNSS 2015)* pp 3841–8